Luminescence from Metallic Quantum Wells in a Scanning Tunneling Microscope

Germar Hoffmann,* Jörg Kliewer,† and Richard Berndt‡

Institut für Experimentelle und Angewandte Physik, Christian-Albrechts-Universität zu Kiel, D-24098 Kiel, Germany

(Received 28 May 2001; published 8 October 2001)

The tunneling current of a scanning tunneling microscope is reported to cause light emission from the metallic quantum well system Na on Cu(111). Optical spectra along with tunneling spectroscopy show that one component of the emission is due to interband transitions between quantum well states of the Na layer. The other component is similar to plasmon-mediated emission observed previously from noble metals. The emission is a unique local probe of the electronic structure of this quantum well system.

DOI: 10.1103/PhysRevLett.87.176803 PACS numbers: 73.20.At, 68.37.Ef, 73.20.Mf, 73.21.Fg

The scanning tunneling microscope (STM) can be used as a source of hot electrons (or holes) to locally, on an atomic scale, prepare electronically or vibrationally excited states. Tunneling spectroscopies of these excitations have made possible, e.g., single molecule vibrational spectroscopy [1] and measurements of electronic lifetimes [2]. This electronic excitation can also lead to luminescence which has been observed from metals, semiconductors, clusters, and molecules with (sub)nanometer lateral resolution [3–10].

Here we report on STM-induced luminescence from ultrathin Na layers on Cu(111). In these overlayers, due to a local band gap of the metal substrate, quantum-well states (QWS) exist close to the Fermi edge, which have been analyzed accurately with angle-resolved, inverse, and two photon photoelectron spectroscopy [11–15]. These QWS are a striking manifestation of electron confinement and thus are ideally suited to investigate the optical properties of a quantum confined metallic system. From these QWS, we observe surprising photon emission characteristics which differ significantly from previous observations on bulk metals. We find well-defined emission lines of substantial intensities which correspond to quantum efficiencies of $\sim 10^{-5}$ photons per tunneling electron. This emission is not due to conventional inverse photoemission processes. We attribute it to interband transitions between two QWS and argue that the excitation process involves tunneling electrons which populate the upper QWS akin to hot electron injection. This mechanism—hot electron injection and an interband transition—appears to differ widely from previous results for metal surfaces. There, inelastic tunneling processes excite a collective excitation, namely, a coupled plasmon of the tip and the sample, which can decay radiatively [3]. The present scenario, however, is reminiscent of the mechanisms involved in luminescence from semiconductor quantum wells.

The sharpness of the QWS emission line [smallest full width at half maximum $\sim$0.17 eV and $\sim$0.28 eV for 0.6 ML (monolayers) and 2 ML, respectively] is not limited by instrument resolution or counting statistics and may be compared to the typical resolution of inverse photoelectron spectroscopy (IPES) ($\sim$0.3 eV) [14,16,17]. In addition to the QWS emission, the fluorescence spectra exhibit emission bands which resemble the plasmon-mediated emission observed previously on pristine noble and transition metal surfaces. Intriguingly, we find two such bands which we attribute to inelastic tunneling from the tip into different QWS of the sample.

The experiments were performed with a custom-built ultrahigh vacuum (UHV) STM operated at a temperature $T = 4.6$ K [18]. Na from a thoroughly outgassed SAES Getters source was dosed onto a Cu(111) crystal that was previously cleaned by repeated sputter and anneal cycles. The evaporation rate was monitored with a quartz crystal microbalance. The quartz data were used as an estimate of the coverage Θ which was further calibrated by the known binding energies of the QWS [11–15]. After preparation at room temperature the sample was transferred to the STM and cooled to $T = 4.6$ K. Following Ref. [19] we define 1 ML as the most densely packed structure of the first Na layer, namely, a $(\frac{3}{2} \times \frac{3}{2})$ mesh. This pattern corresponds to four Na atoms per nine first layer Cu atoms. Tunneling spectra of the differential conductance dI/dV were recorded using a lock-in technique with modulation amplitudes $\sim$5 $\mathrm{mV_{rms}}$ added to the sample bias. For detection of light in the photon energy range $1.2 < h\nu < 3.5$ eV we used a lens system in UHV coupling the light to a grating spectrometer and a liquid nitrogen cooled CCD camera [20]. Compared to previous room temperature investigations an improved detection efficiency enables new modes of measurement which provide a more complete picture of the emission characteristics. In particular, hundreds of fluorescence spectra can be reproducibly recorded while varying the sample voltage over a wide range under computer control. Throughout the measurements we verified that the surface structure was not modified during data acquisition. All experiments were performed repeatedly with several tips.

To characterize the unoccupied electronic states of the Na films we performed dI/dV spectroscopy at positive sample voltage. Figure 1a shows data for 0.6 ML Na where previous IPES data are available for comparison. There are clear features (labeled 1, 2, 3) at energies $E_1 \sim$ 0.4 V, $E_2 \sim 2.0$ V, and $E_3 \sim 2.9$ V with sharper lower

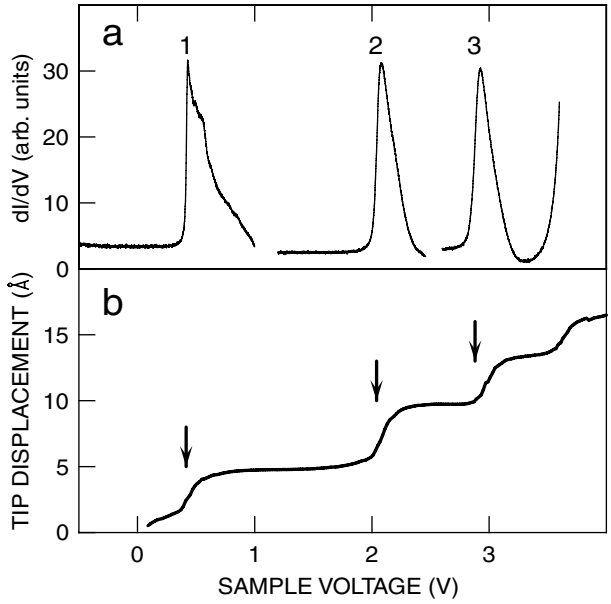

FIG. 1. (a) dI/dV tunneling spectra from 0.6 ML Na on Cu(111) showing three sharp structures which correspond to quantum well states. To cover the wide range of sample voltages, the spectra were recorded consecutively at three different tip-sample distances set by the tunneling parameters prior to opening the STM feedback loop ($I = 1$ nA and $V_s = 1.0, 2.8, 3.6$ V). (b) These states also give rise to rapid increases of the tip-sample distance in constant-current measurements of tip position vs V.

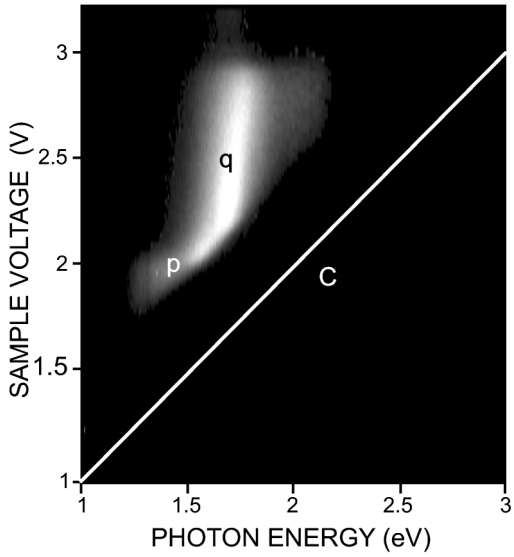

FIG. 2. Series of 100 fluorescence spectra (intensity, represented as a gray scale, vs photon energy $h\nu$) of 0.6 ML Na on Cu(111) recorded at sample voltages V_s from 1.00 to 3.15 V. A strongly dispersing structure and an almost nondispersing emission line are denoted p and q. Line C indicates the quantum cutoff $h\nu = eV_s$.

edges corresponding to the band edges of quantum well states. The lower two quantum well states were previously observed with IPES [14]. Given the limited dynamic range of the current-to-voltage converter used in the experiment, to cover the voltage range of Fig. 1, dI/dV spectra were recorded separately at three different tip-sample distances. Alternatively, these states are easily observed in a "single shot" experiment where the tip-sample distance is measured as a function of V_s under constant-current conditions (Fig. 1b). Each QWS causes an increased tunneling conductance and leads to a rapid increase of the tip-sample distance in the voltage range of the conductance features. Like image states whose exact position is Stark shifted in STM as first demonstrated by Binnig *et al.* [21] the QWS can be affected by the electric field between the tip and the sample. Using the tunneling current I to monitor the tip-sample distance, over two decades of I we find a negligible shift of QWS 1, while state 2 shifts by 0.15 eV over this range.

The photon emission from this quantum well system is characterized in Fig. 2 which shows 100 fluorescence spectra recorded at sample voltages V_s from 1.00 to 3.15 V. At low V_s, emission (denoted p) is observed at small photon energies ($h\nu < 1.6$ eV) with the emission maximum shifting to higher energies as V_s is increased. This emission appears to be similar to plasmon-mediated emission observed from noble metal surfaces due to inelastic tunneling processes [22,23]. A new and unexpected spectral structure (q) emerges at $V_s > 2.1$ V. We find an emission line at $h\nu = 1.7$ eV. Its position is weakly dependent on the gap voltage V_s. This emission corresponds to a quantum efficiency of $\sim 10^{-5}$ photons per electron which is higher than typical values for IPES. Virtually identical data were recorded over many ramps of V_s with the same and several other tunneling tips. The striking absence of a clear influence of the tip shape on its spectral position is a remarkable property of feature q. It contrasts observations from bulk metals where light emission is due to the radiative decay of coupled plasmons of the tip and the sample. In these experiments a distinctive influence of the tip was observed in experiments and calculations [24].

For further analysis, characteristic spectra from Fig. 2 are selected in Fig. 3. At low sample voltage (Fig. 3a, lower graphs) a plasmon resonance p is observed. Remarkably, the high-energy cutoff of the emission is determined by the energy balance $h\nu = eV_s - E_1$ [25] indicating that inelastic tunneling preferentially takes place to the unoccupied lowest QWS 1 at E_1 rather than to the Fermi level. Figure 3b is a simplified energy diagram of the emission mechanism. Electrons tunnel inelastically from occupied tip states to the lowest QWS 1 and give rise to a spectrum of emission with a clear cutoff at high photon energies.

At increased bias the emission q at $h\nu \sim 1.7$ eV (Fig. 3a, hatched peak q) becomes the strongest feature and obscures the plasmon-mediated structure. Comparing the data from Figs. 1 and 3 we find that the photon energy matches the separation between QWS 1 and 2, $h\nu = E_2 - E_1$, indicating that the emission is due to a transition from QWS 2 to QWS 1. The diagram in Fig. 3c

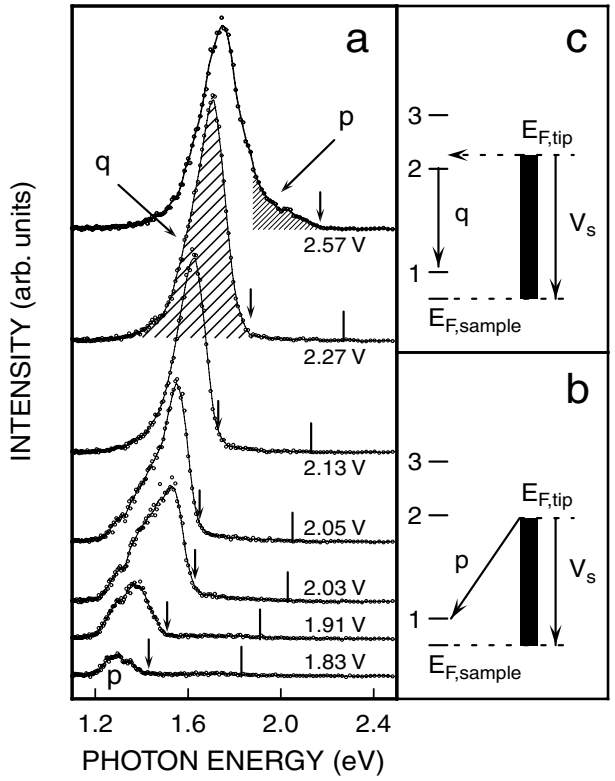

FIG. 3. (a) Selected fluorescence spectra from 0.6 ML Na recorded at various sample voltages V_s indicated on the graphs. Vertical lines and arrows indicate the conditions $h\nu = eV_s$ and $h\nu = eV_s - E_1$, where E_1 is the energy of QWS 1. p and q denote the structures from Fig. 2. (b) Energy diagram of the tip and the sample (1, 2, 3 represent the bottom of QWS 1, 2, and 3) indicating the relevant transition at $V_s < 2.0$ V, where QWS 2 is not accessible. Only plasmon-mediated inelastic tunneling to QWS 1 is observed and causes feature p. (c) At $V_s \geq 2.0$ V, tunneling to QWS 2 starts which results in radiative transition q from this state to QWS 1. This new tunneling channel causes the sharp line at $h\nu = 1.7$ eV.

summarizes the relevant processes. Electrons tunnel elastically from the tip—predominantly from its Fermi level—to QWS 2 of the sample from where a radiative transition to QWS 1 occurs.

The QWS luminescence line is mainly broadened on its high energy side at large V_s. Assuming vertical optical transitions this broadening is consistent with different effective masses of QWS 1 and 2. The observed small shift of peak q at larger V_s reflects the Stark shift of (mainly) QWS 2 by the electric field of the tip [26]. At $V_s = 2.57$ V, a high-energy shoulder appears in the spectra which is consistent with plasmon-type emission (Fig. 3a, hatched shoulder p).

Since the energies of the QWS shift with the Na coverage Θ, we have performed similar spectroscopies for Θ between 0.6 and 2 ML. The results of these experiments are qualitatively similar. In addition to a plasmon-like band, a strong emission occurs at wavelengths given by $h\nu = E_2 - E_1$. These observations further support the emission mechanism proposed above which involves QWS of the sample for the initial and final states.

Figure 4 shows spectra recorded from 2 ML Na. To indicate the reproducibility of the measurements data were shown for an upward and a downward ramp of the sample voltage. Tunneling spectroscopy of the second monolayer (not shown) reveals three density-of-states maxima at $E_1 = 0.15$ eV, $E_2 = 2.2$ eV, and $E_3 = 3.3$ eV which we attribute to quantum well states. The most intriguing features in the optical spectra are maxima Q_{21} at $h\nu = 2.1$ eV and Q_{31} at $h\nu = 3.1$ eV. Their energies match the transition energies $E_2 - E_1$ and $E_3 - E_1$. Moreover, the thresholds for exciting Q_{21} and Q_{31} are $eV_s = E_2$ and $eV_s = E_3$, respectively. Therefore, Q_{21} and Q_{31} can be safely assigned to interband transitions from QWS 2 and 3 to QWS 1 [27]. Next, we observe dispersing features P_1 and P_2. An analysis of their high-energy cutoffs yields $h\nu_1 < eV_s - E_1$ (line C_1 in Fig. 4) and $h\nu_2 < eV_s - E_2$ (line C_2 in Fig. 4). In addition, the exact spectral positions of the maxima of P_1 and P_2 vary from tip to tip, whereas Q_{21} and Q_{31} always occur at the energies given by the sample band structure independent of the tip. Consequently, P_1 and P_2 are attributed to radiative decay of a coupled plasmon of tip and sample which is excited by inelastic tunneling processes from an initial

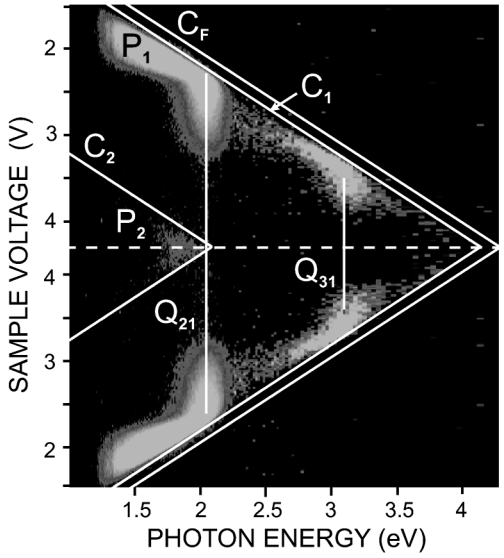

FIG. 4. Series of 250 fluorescence spectra (intensity vs photon energy) of 2.0 ML Na on Cu(111) recorded at sample voltages from 1.5 V up to 4.3 V ($I = 10$ nA) and back down to 1.5 V. The intensities at photon energies $h\nu > 2.3$ eV are scaled by a factor of 10 for clarity. The vertical line denoted by Q_{21} (Q_{31}) marks the photon energy which corresponds to the energy difference between 2nd and 1st (3rd and 1st, respectively) QWS. Lines C_F, C_1, and C_2 indicate the conditions $h\nu = eV_s$, $h\nu = eV_s - E_1$, and $h\nu = eV_s - E_2$, respectively. We attribute features P_1 and P_2 to radiative decay of tip induced plasmon modes via inelastic tunneling into QWS 1 and 2, respectively.

state of the tip to QWS 1 and QWS 2, respectively, as final states. These assignments are also consistent with the observed excitation thresholds. We note that the quantum efficiency of the quantum well luminescence is high and may require that the radiative efficiency be amplified by a resonant process. We tentatively suggest that coupling to localized plasmons may be involved.

In summary, STM-induced luminescence from the metallic quantum well system Na on Cu(111) exhibits unexpected spectral structures. We attribute these structures to radiative transitions between quantum well states of the Na layer which represent a new local probe of these states.

It is a pleasure to thank P. Johansson, J. Aizpurua, and P. Apell for discussions. This work has been supported by the European Commission via the TMR network *EMIT* and the Deutsche Forschungsgemeinschaft via the Schwerpunktsprogramm Elektronentransferprozesse an Grenzflächen.

*Electronic address: hoffmann@physik.uni-kiel.de
†Present address: Infineon, P.O. Box 800949, 81609 München, Germany.
‡Electronic address: berndt@physik.uni-kiel.de

[1] B. C. Stipe, M. A. Rezaei, and W. Ho, Science **280**, 1732 (2000), and references therein.
[2] J. Kliewer *et al.,* Science **266**, 1399 (2000), and references therein.
[3] J. H. Coombs *et al.,* J. Microsc. **152**, 325 (1988).
[4] R. Berndt *et al.,* Phys. Rev. Lett. **74**, 102 (1995).
[5] R. Berndt *et al.,* Science **262**, 1425 (1993).
[6] C. Thirstrup, M. Sakurai, K. Stokbro, and M. Aono, Phys. Rev. Lett. **82**, 1241 (1999).
[7] Y. Uehara, T. Fujita, and S. Ushioda, Phys. Rev. Lett. **83**, 2445 (1999).
[8] N. Nilius, N. Ernst, and H. J. Freund, Phys. Rev. Lett. **84**, 3994 (2000).
[9] G. E. Poirier, Phys. Rev. Lett. **86**, 83 (2001).
[10] P. Renaud and S. F. Alvarado, Phys. Rev. B **44**, 6340 (1991).
[11] S. Å. Lindgren and L. Walldén, Phys. Rev. Lett. **59**, 3003 (1987).
[12] A. Carlsson D. Claesson, S. Å. Lindgren, and L. Walldén, Phys. Rev. Lett. **77**, 346 (1996).
[13] J. M. Carlsson and B. Hellsing, Phys. Rev. B **61**, 13 973 (2000).
[14] R. Dudde, L. S. O. Johansson, and B. Reihl, Phys. Rev. B **44**, 1198 (1991).
[15] N. Fischer, S. Schuppler, R. Fischer, T. Fauster, and W. Steinmann, Phys. Rev. B **43**, 14 722 (1991).
[16] L. Kipp *et al.,* Rev. Sci. Instrum. **68**, 2144 (1997).
[17] T. Fauster *et al.,* Rev. Sci. Instrum. **56**, 1212 (1985).
[18] J. Kliewer, Ph.D. thesis, RWTH Aachen, D-52056, Aachen, Germany, 2000.
[19] D. Tang *et al.,* Surf. Sci. Lett. **255**, L497 (1991).
[20] G. Hoffmann, J. Kröger, and R. Berndt (to be published).
[21] G. Binnig *et al.,* Phys. Rev. Lett. **55**, 991 (1985).
[22] P. Johansson, R. Monreal, and P. Apell, Phys. Rev. B **42**, 9210 (1990).
[23] Y. Uehara, Y. Kimura, S. Ushioda, and K. Takeuchi, Jpn. J. Appl. Phys. **31**, 2465 (1992).
[24] J. Aizpurua, S. P. Apell, and R. Berndt, Phys. Rev. B **62**, 2065 (2000).
[25] J. K. Gimzewski, J. K. Sass, R. R. Schlittler, and J. Schott, Europhys. Lett. **8**, 435 (1989).
[26] G. Hoffmann, P. Johansson, and R. Berndt (to be published).
[27] Close inspection of the 0.6 ML data of Fig. 2 reveals a very weak feature at $h\nu \sim 2.6$ eV consistent with a transition from QWS 3 to QWS 1.